PNAS
www.pnas.org

Supplementary Information for

Evolutionary novelty in the apoptotic pathway of aphids

Mélanie Ribeiro Lopes, Nicolas Parisot, Karen Gaget, Cissy Huygens, Sergio Peignier, Gabrielle Duport, Julien Orlans, Hubert Charles, Pieter Baatsen, Emmanuelle Jousselin, Pedro Da Silva, Korneel Hens, Patrick Callaerts & Federica Calevro

Corresponding authors: Federica Calevro & Patrick Callaerts
Email: federica.calevro@insa-lyon.fr and patrick.callaerts@kuleuven.be

This PDF file includes:

Supplementary Materials and Methods
Figures S1 to S7
Tables S1 to S5
Legends for Datasets S1 and S2

Other supplementary materials for this manuscript include the following:

Datasets S1 and S2

Supplementary Materials and Methods

Phylogenetic reconstruction and protein annotation. For the reconstruction of phylogenetic trees, isolated CASc or BIR domains were aligned using the MAFFT multiple alignment program v7 (https://mafft.cbrc.jp/alignment/server/) and the L-INSI method. Graphical representations of the results were performed with ESPript v3.0 (1). Bayesian phylogenetic inferences were then conducted using MrBayes v3.2.7 (2). We ran two independent analyses with four chains each for 15 million generations, using WAG+I+G4 and WAG models for caspases and IAPs, respectively, as selected by Modeltest using the Bayesian Information Criterion metric (3). The maximum likelihood estimation method, implemented in IQ-TREE v1.6.2 (4), was also used to construct trees from the same data using the same substitution models and 1000 bootstrap replicates. Preliminary phylogenetic analyses, performed using all the retrieved IAP BIR domains, generated four clusters (Fig. S3): (i) cluster 1 includes the BIR_1/2, BIR_1/3 and BIR_2/3 domains from DIAP1/DIAP2-like proteins, (ii) cluster 2 includes the BIR_2/2 and BIR_3/3 from DIAP1/DIAP2-like proteins as well as the BIR domains from single-BIR containing aphid-specific IAPs (i.e. Ap-IAP-C), (iii) cluster 3 includes the BIR domains from dBruce-like proteins and (iv) cluster 4 includes the BIR domains from Deterin-like proteins. As cluster 1 included sequences that were very divergent, we focused only on clusters 2, 3 and 4 for the final phylogenetic analyses (Fig. 2).

Spatio-temporal qRT-PCR analysis. Real-time RT-PCR reactions were performed on a CFX Connect™ Real-Time PCR Detection System (BioRad, Hercules, CA, USA) using 1:5-diluted cDNAs and SYBR Green PCR Master Mix (Roche, Basel, Switzerland) according to the manufacturer's instructions. mRNA levels were quantified relative to the constitutively expressed *rpl7* (NP_001129370.1) gene that was retained by the BestKeeper software tool v1 (5) as the best normalization gene compared with other candidates: *actin* (NP_001119672.1) and *rpl32* (NP_001119682.1). For each aphid life stage analyzed, three independent biological replicates were processed and all qRT-PCR reactions were performed in technical triplicates. Relative expression levels were calculated as previously described (6).

3D Modeling and molecular docking. The stereochemical quality and energy of the aphid modeled BIR domains were evaluated using the PROCHECK software v3.5 (7) and the ProSA (Protein Structure Analysis) server (8), respectively. A representative model of each aphid BIR domain was selected and energy minimized with the Maestro v11.2 software (Schrödinger, LLC, New York, NY, USA). The figures of 3D modeled BIR structures were prepared with the PyMOL molecular Graphics System, v2.0 (Schrödinger, LLC, New York, NY, USA). For the molecular docking step, molecules were refined by energy minimization within Maestro as above. The figures of structural features of the IBM groove of BIR domain binding the tetrapeptide AVPI were displayed with the CCP4mg molecular-graphics software v2.10.11 (9).

Gateway cloning. PCR products were cloned into the pUGa vector using a two-step Gateway cloning protocol. To construct the pUGa vector, the pUAST-attB vector was linearized with EcoRI and XbaI (New England Biolabs, Ipswich, USA), the resulting sticky ends were filled with T4 DNA polymerase (New England Biolabs, Ipswich, USA) and the reading frame B Gateway cassette from the Gateway conversion system (Thermo Fisher Scientific) was ligated in using T4 DNA ligase (New England Biolabs, Ipswich, USA). Gateway cloning was performed by mixing 50 ng of the pDONR221 vector (Thermo Fisher Scientific), 150 ng of the PCR product and 1 µl of BP clonase II enzyme mix (Thermo Fisher Scientific). After incubating for 18 h at 25°C, this mix was transformed into competent One Shot TOP10 cells (Thermo Fisher Scientific) and single colonies were analyzed by colony PCR with M13F and M13R primers using standard protocols. Colonies that gave PCR products of correct size were prepped using the NucleoSpin Plasmid DNA purification kit (Thermo Fisher Scientific), following the manufacturer's instructions, and the plasmids sequenced to select successful entry clones (Source BioScience, Nottingham, UK). The IAP ORFs were subcloned from these entry clones into a pUGa vector by mixing 100 ng of the entry clone, 50 ng of the vector and 1 µl of LR clonase II enzyme mix (Thermo Fisher Scientific). After incubating for 18 h at 25°C, this mix was transformed into competent One Shot TOP10 cells (Thermo Fisher Scientific) and single colonies were analyzed as previously. All successfully subcloned IAPs were prepped and diluted to a final concentration of 100 ng/µl. The plasmid preps were checked again by PCR to verify that no arraying errors were made during prepping.

***Drosophila* eye-based screening assay.** The *Drosophila* eye-based screening assay used in this study was initially developed by Hay *et al.* (10) to confirm the anti-apoptotic role of *Drosophila melanogaster* DIAP1 and DIAP2. Since then, the assay has been used successfully in several studies to assess pro- or anti-apoptotic potential of diverse proteins among which putative caspases (11, 12), IAPs (13, 14), IAP antagonists (15-18) or other apoptosis-related proteins (19-24).

Scanning electron microscopy. Samples for scanning electron microscopy were fixed and stored in 70% EtOH. Samples were then transferred to 100% EtOH, dried using hexamethyldisilazane (HMDS), mounted on stubs and coated with 10nm chrome. Observations were made and images taken on a Zeiss Sigma VP scanning electron microscope (Carl Zeiss Microscopy GmbH, Jena, Germany), operated at 2kV with secondary electron detector under high vacuum, or to suppress charging of the sample, at 10 kV with Variable Pressure Secondary Electron detector at 12 Pascal (N_2-gas).

Supplementary Methods References

1. X. Robert, P. Gouet, Deciphering key features in protein structures with the new ENDscript server. *Nucleic Acids Res.* **42**, W320-324 (2014).

2. J. P. Huelsenbeck, F. Ronquist, R. Nielsen, J. P. Bollback, Bayesian inference of phylogeny and its impact on evolutionary biology. *Science* **294**, 2310-2314 (2001).

3. D. Posada, K. A. Crandall, MODELTEST: testing the model of DNA substitution. *Bioinformatics* **14**, 817-818 (1998).

4. B. Q. Minh *et al*., IQ-TREE 2: New models and efficient methods for phylogenetic inference in the genomic era. *Mol. Biol. Evol.* **37**, 1530-1534 (2020).

5. M. Pfaffl, A. Tichopad, C. Prgomet, T. Neuvians, Determination of stable housekeeping genes, differentially regulated target genes and sample integrity: BestKeeper-Excel-based tool using pair-wise correlations. *Biotechnol. Letters* **26**, 509-515 (2004).

6. P. Sapountzis *et al*., New insight into the RNA interference response against cathepsin-L gene in the pea aphid, *Acyrthosiphon pisum*: molting or gut phenotypes specifically induced by injection or feeding treatments. *Insect Biochem. Mol. Biol.* **51**, 20-32 (2014).

7. R. A. Laskowski, J. A. Rullmannn, M. W. MacArthur, R. Kaptein, J. M. Thornton, AQUA and PROCHECK-NMR: programs for checking the quality of protein structures solved by NMR. *J. Biomol. NMR* **8**, 477-486 (1996).

8. M. Wiederstein, M. J. Sippl, ProSA-web: interactive web service for the recognition of errors in three-dimensional structures of proteins. *Nucleic Acids Res.* **35**, W407-410 (2007).

9. S. McNicholas, E. Potterton, K. S. Wilson, M. E. Noble, Presenting your structures: the CCP4mg molecular-graphics software. *Acta Crystallogr. D. Biol. Crystallogr.* **67**, 386-394 (2011).

10. B. A. Hay, D. A. Wassarman, G. M. Rubin, *Drosophila* homologs of baculovirus inhibitor of apoptosis proteins function to block cell death. *Cell* **83**, 1253-1262 (1995).

11. P. Meier, J. Silke, S. J. Leevers, G. I. Evan, The *Drosophila* caspase DRONC is regulated by DIAP1. *EMBO J.* **19,** 598-611(2000).

12. N. L. Harvey *et al.,* Characterization of the *Drosophila* caspase, DAMM. *J. Biol. Chem.* **276,** 25342-25350 (2001).

13. R. Wilson *et al*., The DIAP1 RING finger mediates ubiquitination of Dronc and is indispensable for regulating apoptosis. *Nat. Cell. Biol.* **4,** 445-450 (2002).

14. C. Domingues, H. D. Ryoo, *Drosophila* BRUCE inhibits apoptosis through non-lysine ubiquitination of the IAP-antagonist REAPER. Cell Death Differ. **19,** 470-477 (2012).

15. J. P. Wing, M. Schwartz, J. R. Nambu, The RHG motifs of *Drosophila* Reaper and Grim are important for their distinct cell death-inducing abilities. *Mech. Dev.* **102,** 193-203 (2001).

16. T. Tenev, A. Zachariou, R. Wilson, A. Paul, P. Meier, Jafrac2 is an IAP antagonist that promotes cell death by liberating Dronc from DIAP1. *EMBO J.* **21**, 5118-5129 (2002).

17. J. P. Wing *et al*., *Drosophila* sickle is a novel grim-reaper cell death activator.*Curr. Biol.* **12,** 131-135 (2002).

18. F. S. Khan *et al*., The interaction of DIAP1 with dOmi/HtrA2 regulates cell death in *Drosophila. Cell Death Differ.* **15**, 1073-1083 (2008).

19. T. Igaki *et al*., Eiger, a TNF superfamily ligand that triggers the *Drosophila* JNK pathway. *EMBO J.* **21**, 3009-3018 (2002).

20. M. Mallik, S. C. Lakhotia, The developmentally active and stress-inducible noncoding hsromega gene is a novel regulator of apoptosis in *Drosophila*. *Genetics* **183,** 831-852 (2009).

21. J. P. Ribaya *et al.*, The deubiquitinase emperor's thumb is a regulator of apoptosis in *Drosophila*. *Dev. Biol.* **329,** 25-35 (2009).

22. J. A.Schoenherr *et al.*, *Drosophila* activated Cdc42 kinase has an anti-apoptotic function. *PLoS Genet.* **8,** e1002725 (2012).

23. S. A. Sinenko, Proapoptotic function of deubiquitinase DUSP31 in *Drosophila*. *Oncotarget* **8**, 70452-70462 (2017).

24. A. Kumar, A. K. Tiwari, Molecular chaperone Hsp70 and its constitutively active form Hsc70 play an indispensable role during eye development of *Drosophila melanogaster*. *Mol. Neurobiol.* **55**, 4345-4361 (2018).

Supplementary Figures

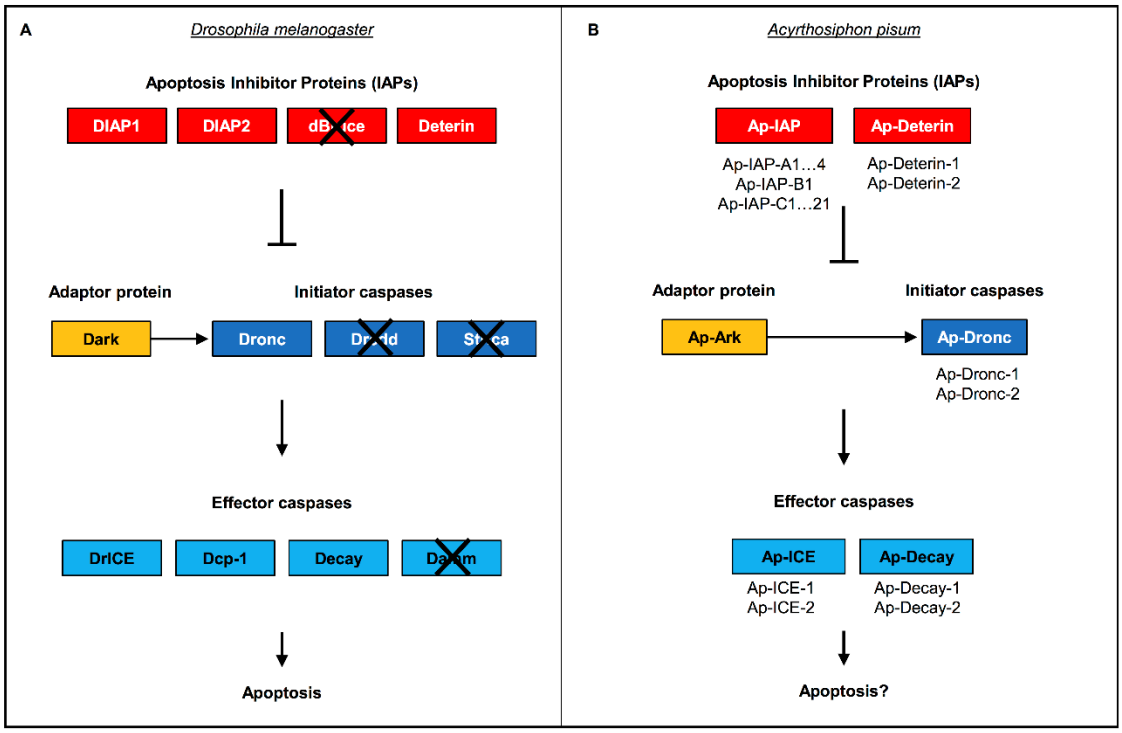

Figure S1. The apoptotic pathways in the fruit fly and pea aphid genomes. Schematic overview of the apoptotic pathways in *Drosophila melanogaster* (**A**) and *Acyrthosiphon pisum* (**B**). Several proteins of *D. melanogaster* (the inhibitor dBruce and the caspases Dredd, Strica and Damm, indicated by black cross) do not have homologs in *A. pisum*. Genes encoding other proteins have undergone multiple duplications that notably led to a significant expansion of the IAP family. Paralogs were given the same name and numbered to facilitate their identification. They are listed underneath the box containing their common name.

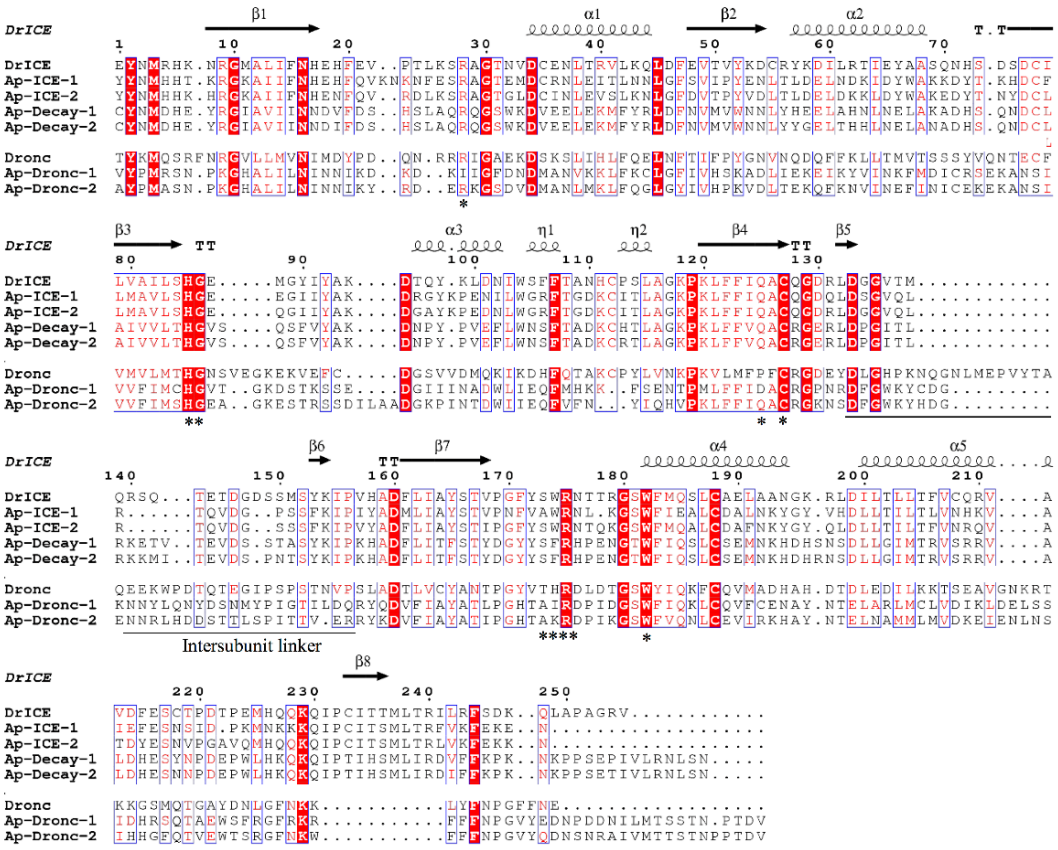

Figure S2. Pea aphid caspases contain the residues necessary for their proteolytic action. The sequence alignment of CASc domains from *Acyrthosiphon pisum* and *Drosophila melanogaster* caspases shows conserved motifs (highlighted in red when fully conserved, written in red when partially conserved). Residues involved in substrate recognition and catalysis are marked (*). The portions of sequence found upstream and downstream of the indicated inter-subunit linker correspond to the p20 and p10 subunits, respectively. When several transcripts were available, the longest one was selected for alignment. The corresponding secondary structure (arrow, β-strand; helix, α-helix) is reported in black above the alignment (DrICE as a reference).

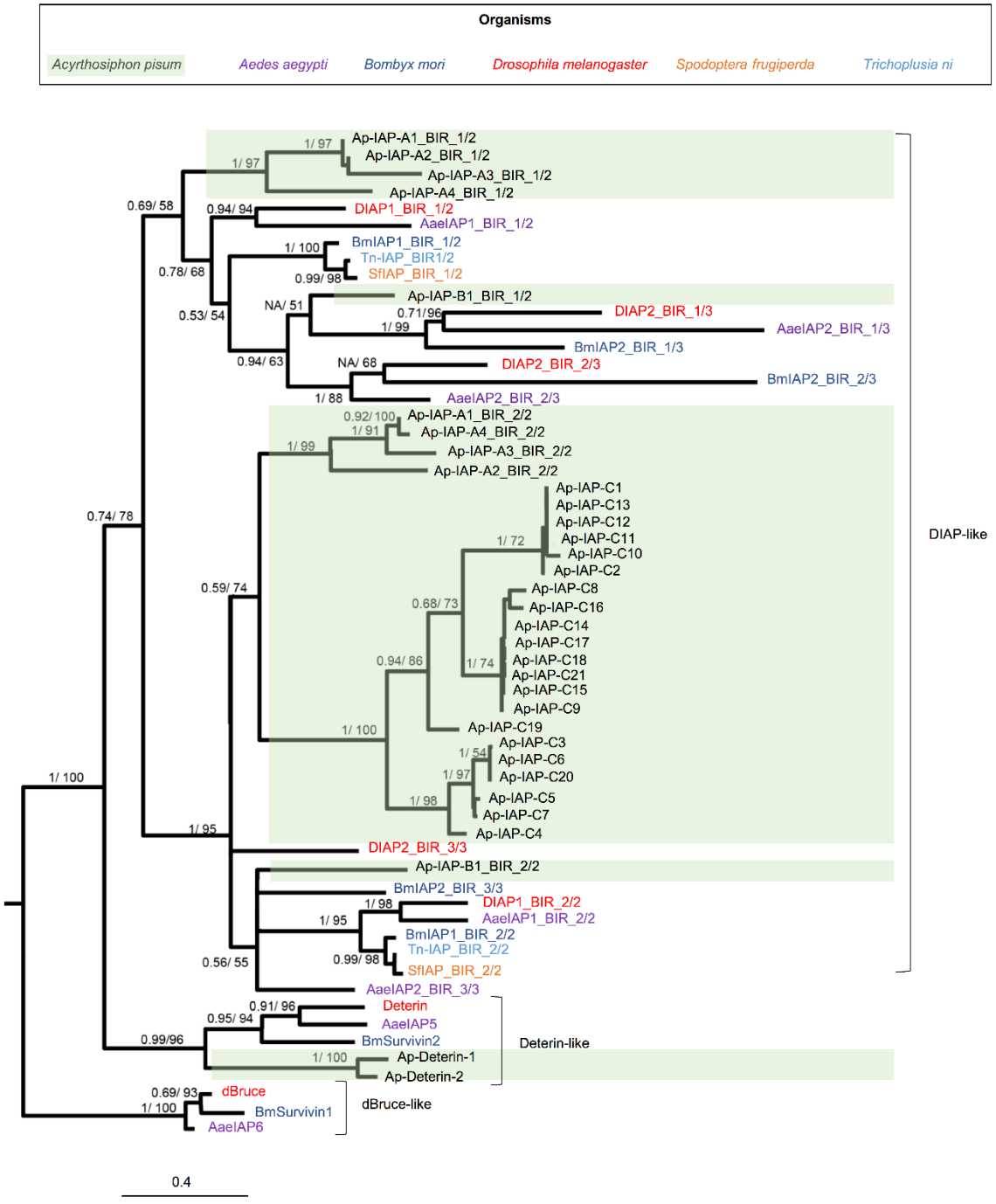

Figure S3. Phylogenetic relationships between IAP sequences found in *Acyrthosiphon pisum* and their counterparts in different insects. A phylogenetic reconstruction was conducted using the complete set of isolated BIR domains of IAPs from the insects *Acyrthosiphon pisum*, *Aedes aegypti*, *Bombyx mori*, *Drosophila melanogaster*, *Spodoptera frugiperda* and *Trichoplusia ni*. When an IAP possesses several BIR domains, they are numbered to differentiate them (e.g. BIR_1/2, BIR_2/2). For each node, Bayesian posterior probability and bootstrap values are indicated. Midpoint rooting was used to present the tree.

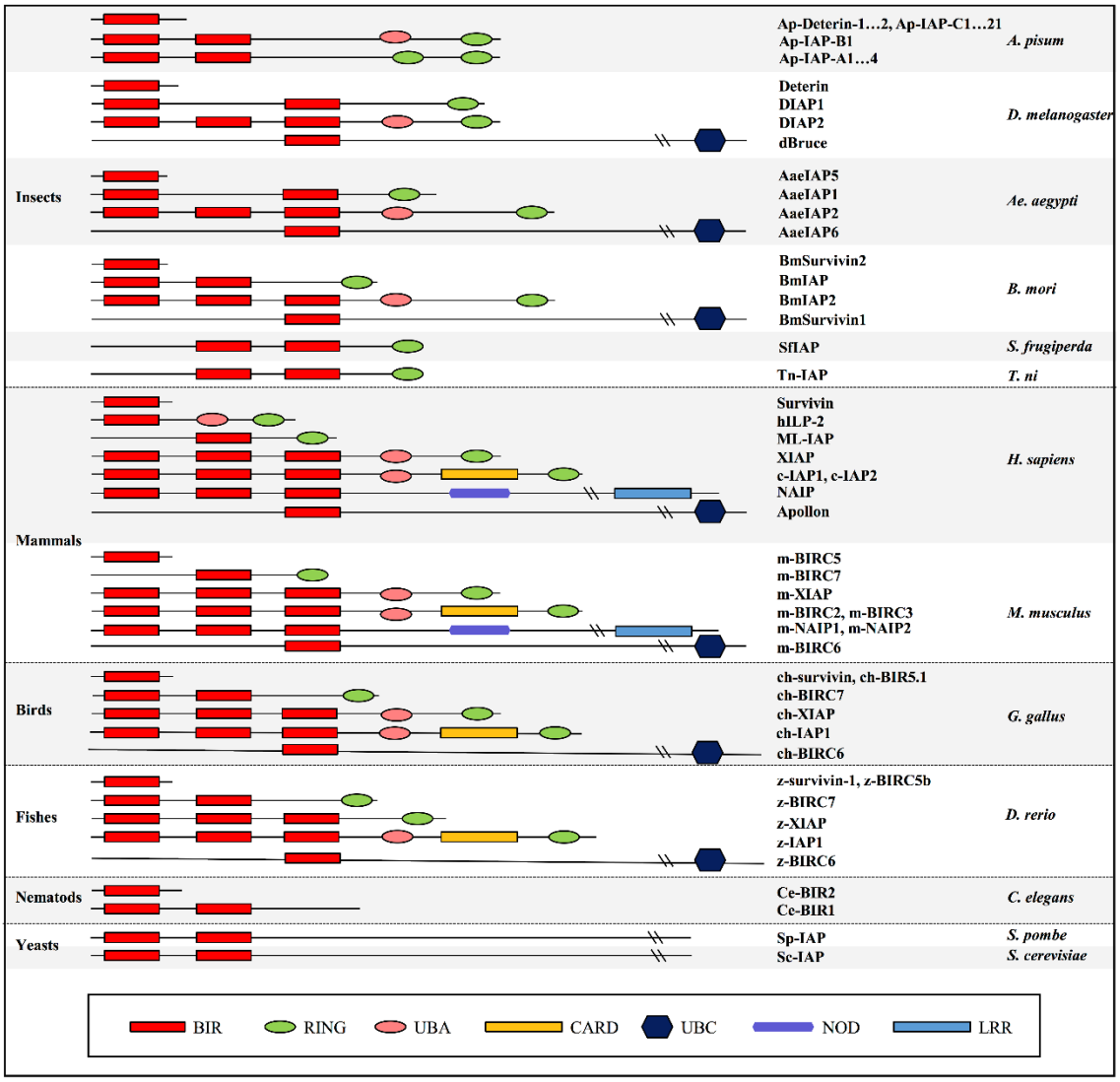

Figure S4. Emergence of new structures in the pea aphid IAPs. Domain composition of IAP proteins from different species (*Acyrthosiphon pisum, Drosophila melanogaster, Aedes aegypti, Bombyx mori, Spodoptera frugiperda, Trichoplusia ni, Homo sapiens, Mus musculus, Gallus gallus, Danio rerio, Caenorhabditis elegans, Schizosaccharomyces pombe* and *Saccharomyces cerevisiae*). Pea aphid IAPs present a limited structural diversity despite their important number: they contain two BIR domains at most and are completely devoid of UBC domain, consistent with the absence of a dBruce homolog in the pea aphid genome. However, the pea aphid is the only organism in which IAPs with two RING domains have been identified. BIR domains (Baculoviral IAP Repeat; ID: IPR001370), characteristics of the IAP protein family, are represented by a red rectangle, RING domains (Really Interesting New Gene) by a green oval, UBA domains (Ubiquitin Associated domains) by a pink oval, CARD domains (CAspase Recruitment Domain) by a pink rectangle, UBC domains (Ubiquitin-Conjugating Enzymes) by a blue hexagon, NOD domains (Nucleotide Oligomerization Domain) by a purple rectangle and LRR (Leucine Rich Repeat;) by a blue rectangle.

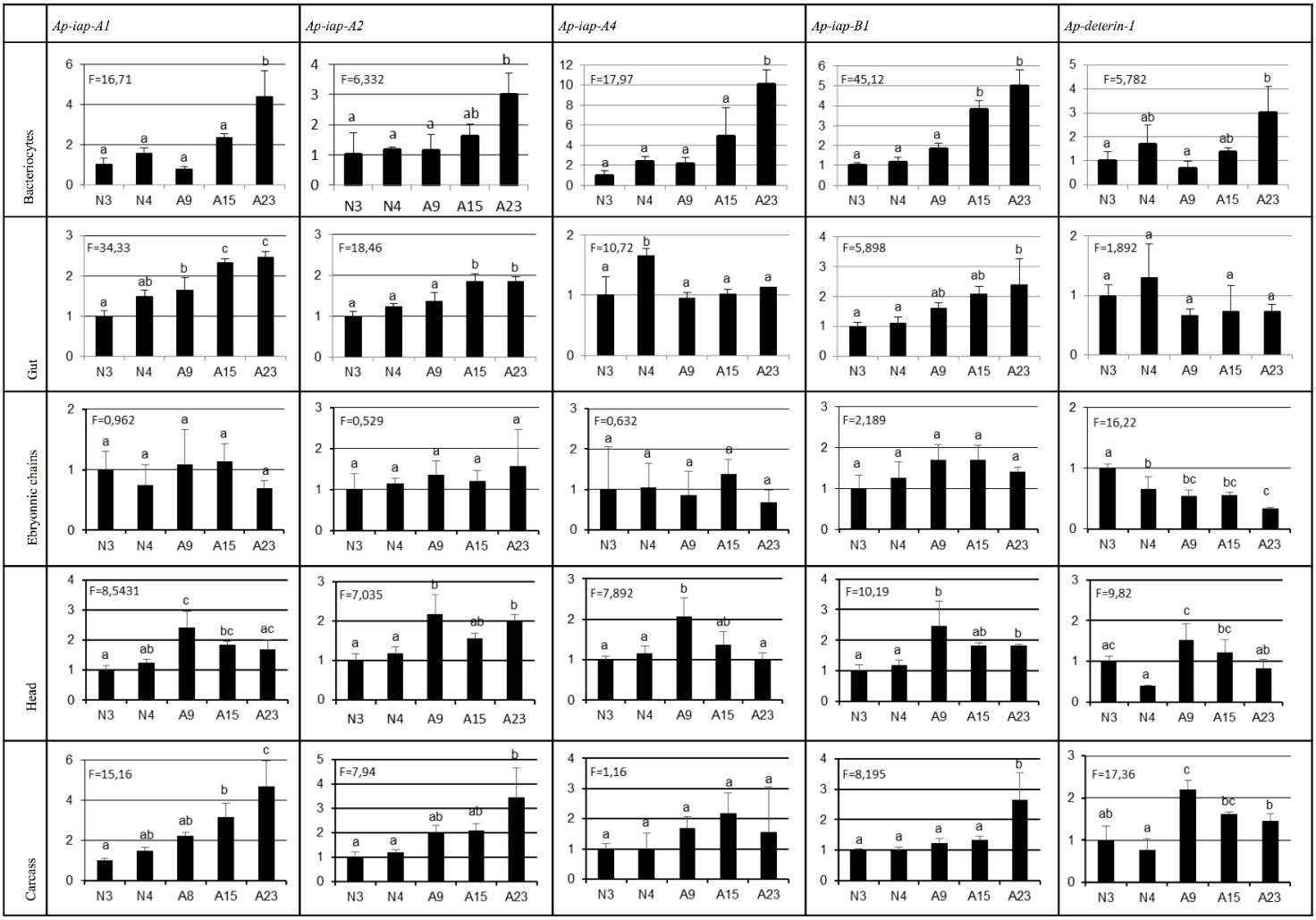

Figure S5. Expression levels of bacteriocyte-specific *Ap-iaps* in different tissues throughout aphid development. The expression levels were measured in five different tissues (bacteriocytes, gut, embryonic chains, head and carcass) and at five different development stages (N3 and N4: 3rd and 4th nymphal instars, respectively; A9, A15 and A23: adults at stages 9, 15 and 23, respectively), based on qRT-PCR data analysis. IAP gene-expression levels in the different tissues are expressed relative to the third-instar nymph levels and the *rpl7* gene was used for data normalization. Data are presented as means±SD from three independent biological replicates. Data were analyzed by one-way ANOVA followed by a post hoc multiple-comparisons test (Tukey's HSD test). Life stages labeled with different letters are significantly different ($P < 0.05$). ANOVA F values are indicated on each graph.

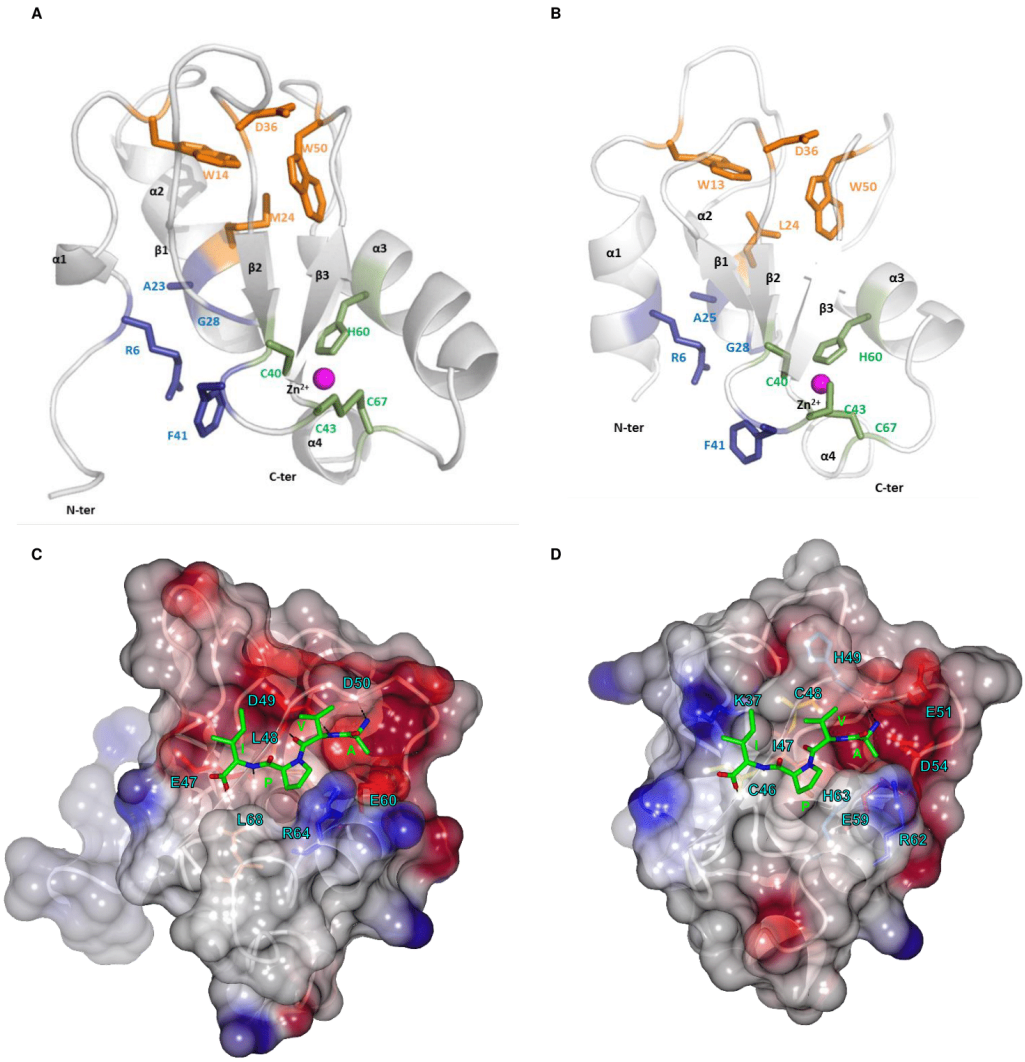

Figure S6. 3D structure and secondary structure predictions of BIR1 domains in Ap-Deterin-1 and Ap-IAP-B1. **A** 3D modeled structure prediction of Ap-Deterin-1_BIR1 domain with focus on the three structural padlocks stabilizing the BIR specific zinc chelating fold: (i) the first Zn^{2+} (magenta) binding residue C40-C43-H60-C67 padlock in green sticks, (ii) the second R6-A25-G28-F41 padlock in blue sticks and (iii) the third W14-M24-D36-W50 padlock in orange sticks. **B** 3D modeled structure prediction of Ap-IAP-B1_BIR1 domain with focus on the three structural padlocks stabilizing the BIR specific zinc chelating fold: (i) the first Zn^{2+} (magenta) binding residue C40-C43-H60-C67 padlock in green sticks, (ii) the second R6-A25-G28-F41 padlock in blue sticks and (iii) the third W14-L24-D36-W50 padlock in orange sticks. **C** Structural features of the predicted IBM groove of the Ap-Deterin-1_BIR1 domain binding the tetrapeptide AVPI (in green stick). The electrostatic surface of Ap-Deterin-1_BIR1 domain is represented with the negatively and positively charged regions highlighted in red and blue, respectively. Only the residues interacting with AVPI are represented as colored sticks and labeled. Hydrogen bonds anchoring the tetrapeptide AVPI in the IBM groove are represented as black dashes. **D** Structural features of the predicted IBM groove of the Ap-IAP-

B1_BIR1 domain binding the tetrapeptide AVPI (in green stick). The electrostatic surface of Ap-IAP-B1_BIR1 domain is represented with the negatively and positively charged regions highlighted in red and blue, respectively. Only the residues interacting with AVPI are represented as colored sticks and labeled. Hydrogen bonds anchoring the tetrapeptide AVPI in the IBM groove are represented as black dashes.

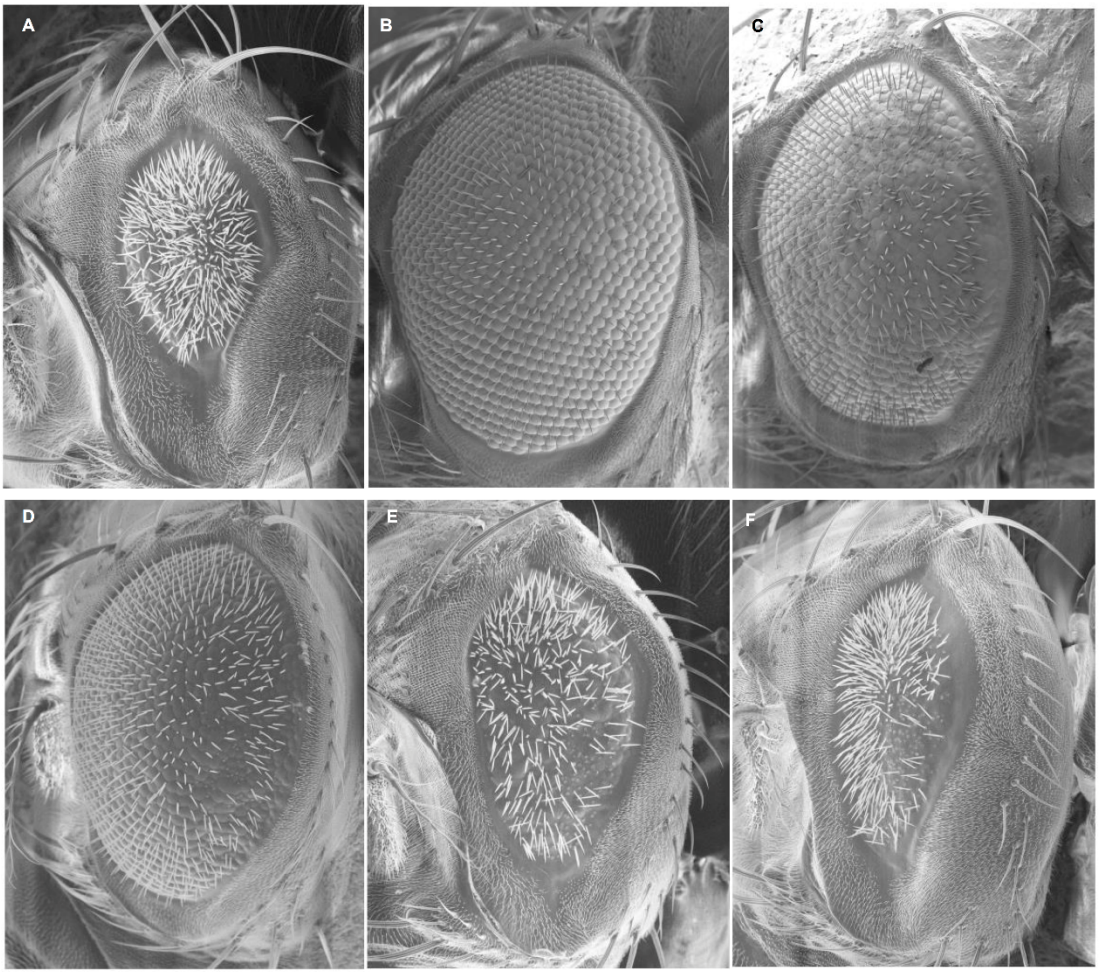

Figure S7. Ap-IAPs are able to rescue induced apoptosis in *Drosophila* eyes in *in vivo* experiments. A SEM picture of a control fly eye in which the apoptosis inducer gene *rpr* is continuously expressed. Imaging of eyes from different *Drosophila melanogaster* transgenic lines showed that the GMR-*rpr*-dependent small eye phenotype is nearly completely suppressed by coexpression of *Ap-iap-A1* (**B**), *Ap-iap-A2* (**C**) and *Ap-iap-A4* (**D**), while coexpression of *Ap-iap-B1* (**E**) and *Ap-deterin-1* (**F**) only partially suppress this phenotype. Nominal magnification in all images is 500x.

Supplementary Tables

Table S1. Annotation of the complete repertoire of pea aphid apoptosis related proteins.

	Name	NCBI Accession number	Predicted transcripts	Length (AA)	Conserved domains
Adaptor protein	Ap-Ark	LOC100571592	2	1345	CARD, NB-ARC, WD40 REPEAT
Caspases	Ap-Dronc-1	LOC100571705	3	413	CARD, CASc
	Ap-Dronc-2	LOC100569019	4	411	CARD, CASc
	Ap-ICE-1	LOC100162302	1	315	CASc
	Ap-ICE-2	LOC100160647	2	312-286	CASc
	Ap-Decay-1	LOC100161906	4	459-448	CASc
	Ap-Decay-2	LOC115034111	1	272	CASc
IAPs	Ap-Deterin-1	Det	2	159-130	BIR
	Ap-Deterin-2	LOC100569400	1	157	BIR
	Ap-IAP-A1	LOC103310098	5	526-466	BIR (2), RING (2)
	Ap-IAP-A2	LOC100159652	1	415	BIR (2), RING (2)
	Ap-IAP-A3	LOC100168361	1	455	BIR (2), RING (2)
	Ap-IAP-A4	LOC100168556	1	482	BIR (2), RING (2)
	Ap-IAP-B1	LOC100159034	1	530	BIR (2), RING, UBA
	Ap-IAP-C1	LOC103309101	1	227	BIR
	Ap-IAP-C2	LOC103311428	1	170	BIR
	Ap-IAP-C3	LOC107882438	1	160	BIR
	Ap-IAP-C4	LOC115034795	1	159	BIR
	Ap-IAP-C5	LOC115034796	1	159	BIR
	Ap-IAP-C6	LOC115034872	1	159	BIR
	Ap-IAP-C7	LOC115035070	1	142	BIR
	Ap-IAP-C8	LOC103309011	1	134	BIR
	Ap-IAP-C9	LOC103311764	1	133	BIR
	Ap-IAP-C10	LOC103310572	1	132	BIR
	Ap-IAP-C11	LOC103310750	1	132	BIR
	Ap-IAP-C12	LOC115034852	1	132	BIR
	Ap-IAP-C13	LOC115035087	1	132	BIR
	Ap-IAP-C14	LOC103307944	1	131	BIR
	Ap-IAP-C15	LOC103308123	1	131	BIR
	Ap-IAP-C16	LOC103309299	1	131	BIR
	Ap-IAP-C17	LOC103310748	1	131	BIR
	Ap-IAP-C18	LOC115033401	1	131	BIR
	Ap-IAP-C19	LOC100570215	1	128	BIR
	Ap-IAP-C20	LOC107885648	1	128	BIR
	Ap-IAP-C21	LOC107883770	1	123	BIR

Putative pea aphid apoptosis related proteins are listed with the names they were attributed in this study. When more than one domain is present in the putative protein, the number is specified between brackets. Abbreviations: CARD: CAspase Recruitment Domain; NB-ARC: Nucleotide-Binding Adaptor shared by APAF-1, R proteins, and CED-4; CASc, CASpase catalytic domain; BIR, Baculoviral IAP Repeat; RING, Really Interesting New Gene; UBA, Ubiquitin-Associated domain.

.

Table S2. Complete repertoire of adaptor and caspase proteins in the aphid lineage.

Species	NCBI Accession number	AphidBase Accession number	Predicted transcripts	Length (AA)	Conserved domains
Aphis glycines	/	**AG004743**	1	408	CARD, CASc
	/	**AG014444**	1	399	CARD, CASc
	/	**AG002421**	1	1235	CASc
	/	AG005720	1	314	CASc
Aphis gossypii	**LOC114126303**	/	3	408	CARD, CASc
	LOC114119019	/	1	397	CARD, CASc
	LOC114129378	/	2	456	CASc
Cinara cedri	**VVC43788**	/	1	413	CARD, CASc
	VVC33137	/	1	465	CASc
	VVC43315	/	2	318-245	CASc
Daktulospheira vitifoliae	/	**DV3013013**	1	439	CARD, CASc
	/	**DV3011341**	1	450	CASc
	/	DV3008404	1	306	CASc
	/	DV3008405	1	292	CASc
Diuraphis noxia	**LOC107166680**	/	3	413	CARD, CASc
	LOC107162114	/	3	459	CASc
	LOC107168420	/	1	312	CASc
Melanaphis sacchari	**LOC112595911**	/	2	408	CARD, CASc
	LOC112604125	/	2	456	CASc
	LOC112597794	/	2	328-314	CASc
Myzus cerasi	/	**Mca20791**	1	413	CARD, CASc
	/	Mca23190	1	305	CASc
	/	Mca28408	1	165	CASc
	/	Mca26483	1	165	CASc
	/	Mca05862	1	158	CASc
Myzus persicae	**LOC111038906**	/	2	414	CARD, CASc
	LOC111042739	/	1	415	CARD, CASc
	LOC111038323	/	4	465	CASc
	LOC111029969	/	1	312	CASc
Rhopalosiphum maidis	**LOC113547787**	/	2	409	CARD, CASc
	LOC113551225	/	4	457	CASc
	LOC113557886	/	1	386	CASc
	LOC113550549	/	1	314	CASc
Rhopalosiphum padi	/	**g12615**	1	410	CARD, CASc
	/	**g18354**	1	398	CARD, CASc
	/	**g20133**	1	398	CARD, CASc
	/	**g6358**	1	458	CASc
	/	**g6029**	1	386	CASc
Sipha flava	**LOC112682086**	/	1	403	CARD, CASc
	LOC112682730	/	3	454	CASc
	LOC112687160	/	1	310	CASc
	LOC112687159	/	1	272	CASc

Genes encoding proteins with a long prodomain of more than 100 amino acids (putative initiator capsases) are written in bold and underlined. Abbreviations: CARD: CAspase Recruitment Domain; CASc, CASpase catalytic domain.

Table S3. Complete repertoire of IAPs in the aphid lineage.

Species	NCBI Accession number	AphidBase Accession number	Predicted transcripts	Size (AA)	Conserved domains
Aphis glycines	/	AG006812	1	618	BIR (5), RING (2)
	/	AG017437	1	438	BIR (5)
	/	AG012793	1	635	BIR (4), RING (3)
	/	AG013373	1	476	BIR (3), RING (2)
	/	AG015575	1	461	BIR (3), RING
	/	AG007395	1	482	BIR (2), RING (2)
	/	AG007064	1	476	BIR (2), RING (2)
	/	AG017243	1	410	BIR (2), RING (2)
	/	AG007394	1	566	BIR (2), RING
	/	AG018494	1	360	BIR (2), RING
	/	AG019006	1	355	BIR (2), RING
	/	AG018229	1	271	BIR (2), RING
	/	AG017012	1	337	BIR (2)
	/	AG018513	1	312	BIR (2)
	/	AG018191	1	213	BIR (2)
	/	AG009711	1	501	BIR, RING
	/	AG013324	1	338	BIR
	/	AG017296	1	219	BIR
	/	AG017365	1	219	BIR
	/	AG011999	1	164	BIR
	/	AG010471	1	159	BIR
	/	AG013679	1	156	BIR
	/	AG012752	1	132	BIR
	/	AG012794	1	122	BIR
	/	AG018976	1	110	BIR
	/	AG018327	1	80	BIR
Aphis gossypii	LOC114130948	/	1	618	BIR (5), RING (2)
	LOC114131776	/	1	241	BIR (3)
	LOC114120528	/	1	512	BIR (2), RING (2)
	LOC114121048	/	1	482	BIR (2), RING (2)
	LOC114121448	/	1	376	BIR (2), RING (2)
	LOC114121047	/	1	503	BIR (2), RING, UBA
	LOC114121450	/	1	150	BIR (2)
	LOC114127554	/	1	301	BIR, RING
	LOC114126338	/	1	243	BIR
	LOC114119937	/	1	159	BIR
Cinara cedri	VVC38797	/	1	716	BIR (2), RING (2)
	VVC41444	/	2	575-431	BIR (2), RING (2)
	VVC34545	/	2	477-450	BIR (2), RING (2)
	VVC24365	/	3	474-458	BIR (2), RING (2)
	VVC46145	/	1	445	BIR (2), RING (2)
	VVC29531	/	1	433	BIR (2), RING (2)
	VVC24368	/	1	531	BIR (2), RING, UBA
	VVC29856	/	1	156	BIR
	VVC41669	/	1	156	BIR
	VVC33236	/	1	151	BIR
	VVC44076	/	1	131	BIR
	VVC26684	/	1	97	BIR

Daktulospheira vitifoliae	/	DV3009948	1	483	BIR (2), RING (2)
	/	DV3009949	1	484	BIR (2), RING, UBA
	/	DV3016500	1	171	BIR (2)
	/	DV3014705	1	171	BIR (2)
	/	DV3008798	1	432	BIR
	/	DV3022113	1	366	BIR
	/	DV3016501	1	237	BIR
	/	DV3006888	1	157	BIR
	/	DV3008759	1	153	BIR
	/	DV3023284	1	143	BIR
	/	DV3003143	1	139	BIR
	/	DV3014638	1	139	BIR
	/	DV3017300	1	138	BIR
	/	DV3021476	1	137	BIR
	/	DV3023181	1	134	BIR
	/	DV3019768	1	132	BIR
	/	DV3017336	1	129	BIR
	/	DV3020822	1	124	BIR
	/	DV3021159	1	121	BIR
	/	DV3002495	1	120	BIR
	/	DV3019788	1	120	BIR
	/	DV3019024	1	119	BIR
	/	DV3018103	1	109	BIR
	/	DV3012104	1	109	BIR
	/	DV3003461	1	106	BIR
	/	DV3011323	1	100	BIR
	/	DV3004969	1	76	BIR
	/	DV3021895	1	67	BIR
	/	DV3020843	1	62	BIR
	/	DV3000295	1	61	BIR
	/	DV3011561	1	49	BIR
Diuraphis noxia	LOC107166234	/	4	477-466	BIR (2), RING (2)
	LOC107173012	/	1	466	BIR (2), RING (2)
	LOC107165677	/	1	458	BIR (2), RING (2)
	LOC107166235	/	1	257	BIR (2)
	LOC107168615	/	1	159	BIR
	LOC107170930	/	1	98	BIR
Melanaphis sacchari	LOC112600252	/	1	491	BIR (3), RING (2)
	LOC112592348	/	1	473	BIR (3), RING (2)
	LOC112600254	/	1	460	BIR (3), RING (2)
	LOC112590851	/	3	485-474	BIR (2), RING (2)
	LOC112600020	/	1	465	BIR (2), RING (2)
	LOC112590850	/	1	496	BIR (2), RING
	LOC112604327	/	1	159	BIR
	LOC112593942	/	1	149	BIR
	LOC112598371	/	1	135	BIR
	LOC112592002	/	1	134	BIR
	LOC112592448	/	1	134	BIR
	LOC112593875	/	1	134	BIR
	LOC112594694	/	1	134	BIR
	LOC112596504	/	1	134	BIR
	LOC112603410	/	1	134	BIR
	LOC112600360	/	1	120	BIR
	LOC112592222	/	1	107	BIR
	LOC112591322	/	1	90	BIR

	LOC112593863	/	1	90	BIR
Myzus cerasi	/	Mca10116	1	557	BIR (4), RING (2)
	/	Mca10160	1	468	BIR (2), RING (2)
	/	Mca19538	1	460	BIR (2), RING (2)
	/	Mca15052	1	492	BIR (2), RING, UBA
	/	Mca17716	1	213	BIR, RING
	/	Mca18774	1	257	BIR
	/	Mca00372	1	158	BIR
	/	Mca17715	1	148	BIR
	/	Mca21955	1	138	BIR
Myzus persicae	LOC111039944	/	1	557	BIR (4), RING (2)
	LOC111027568	/	4	479-468	BIR (2), RING (2)
	LOC111039746	/	1	460	BIR (2), RING, UBA
	LOC111027549	/	6	521-497	BIR (2), RING, UBA
	LOC111032732	/	1	498	BIR, RING
	LOC111028900	/	1	174	BIR
	LOC111042344	/	1	160	BIR
	LOC111037378	/	2	159	BIR
	LOC111040353	/	1	159	BIR
	LOC111026657	/	1	151	BIR
	LOC111038800	/	1	145	BIR
	LOC111033785	/	1	138	BIR
	LOC111026214	/	1	133	BIR
	LOC111026337	/	1	133	BIR
	LOC111026737	/	1	133	BIR
	LOC111027498	/	1	133	BIR
	LOC111039762	/	1	133	BIR
	LOC111040897	/	1	123	BIR
	LOC111027266	/	1	112	BIR
	LOC111041131	/	1	104	BIR
	LOC111041395	/	1	104	BIR
Rhopalosiphum maidis	LOC113558592	/	1	517	BIR (3), RING (2)
	LOC113557951	/	1	499	BIR (3), RING (2)
	LOC113557944	/	1	473	BIR (3), RING (2)
	LOC113558506	/	1	470	BIR (3), RING (2)
	LOC113558071	/	1	361	BIR (3)
	LOC113559418	/	1	491	BIR (2), RING (2)
	LOC113556324	/	3	482-471	BIR (2), RING (2)
	LOC113553059	/	2	482-471	BIR (2), RING (2)
	LOC113556228	/	1	506	BIR (2), RING, UBA
	LOC113558419	/	3	581-447	BIR (1), RING (2)
	LOC113554160	/	2	159	BIR
	LOC113559037	/	1	96	BIR
Rhopalosiphum padi	/	g26140	1	545	BIR (4), RING (2)
	/	g11402	1	524	BIR (3), RING (2)
	/	g10703	1	492	BIR (3), RING (2)
	/	g23251	1	472	BIR (3), RING
	/	g11401	1	311	BIR (3)
	/	g10367	1	595	BIR (2), RING (2)
	/	g15101	1	495	BIR (2), RING (2)
	/	g10369	1	507	BIR (2), RING, UBA
	/	g20480	1	511	BIR, RING (2)
	/	g19135	1	546	BIR
	/	g12191	1	504	BIR

	/	g23890	1	327	BIR
	/	g16933	1	177	BIR
	/	g12803	1	176	BIR
	/	g24927	1	170	BIR
	/	g22618	1	166	BIR
	/	g20895	1	135	BIR
	/	g20025	1	135	BIR
	/	g23385	1	134	BIR
	/	g14956	1	134	BIR
Sipha flava	LOC112686708	/	1	551	BIR (2), RING (2)
	LOC112686705	/	5	470	BIR (2), RING (2)
	LOC112688984	/	1	240	BIR (2)
	LOC112681260	/	1	281	BIR (1), RING (2)
	LOC112684840	/	1	160	BIR
	LOC112683532	/	1	150	BIR
	LOC112680278	/	1	129	BIR
	LOC112681261	/	1	119	BIR
	LOC112685876	/	1	112	BIR
	LOC112679781	/	1	105	BIR

When more than one domain is present, the number is specified between brackets. Abbreviations: BIR, Baculoviral IAP Repeat ; RING, Really Interesting New Gene; UBA, Ubiquitin-Associated domain.

Table S4. Caspases and IAP sequences used for pea aphid proteins identification and phylogenetic reconstruction.

Insect order	Species	Protein name	NCBI identifier
Caspases			
Diptera	*Drosophila melanogaster*	Dronc	NP_524017.1
		Dredd	NP_477249.3
		Strica	NP_610193.1
		DrICE	NP_524551.2
		Dcp-1	NP_476974.1
		Decay	NP_477462.1
		Damm	NP_523703.2
	Aedes aegypti	AaeDronc	XP_001655433.2
		AaeDredd	XP_021711617.1
		AaeCASPS7	XP_021704883.1
		AaeCASPS8	XP_001648537.2
		AaeCASPS15/16	XP_021709830.1
		AaeCASPS17	XP_021709833.1
		AaeCASPS18	XP_001656810.1
		AaeCASPS19	XP_001656809.1
		AaeCASPS20	XP_021694895.1
		AaeCASPS21	XP_021709829.1
Lepidoptera	*Bombyx mori*	BmDronc	NP_001182396.1
		BmDredd	NP_001108337.1
		BmICE-1	NP_001037297.1
		BmICE-5	NP_001106741.1
		BmCaspase-1	NP_001037050.1
		BmCaspase-N	NP_001243935.1
	Helicoverpa armigera	Ha-caspase-1	XP_021183524.1
	Spodoptera frugiperda	Sf-caspase-1	P89116.1
		SfDronc	AGG91491.1
		SfDredd	AMR71144.1
	Trichoplusia ni	Tn-caspase-1	XP_026742653.1
Hemiptera	*Bemisia tabaci*	Bt-caspase-1	XP_018897656.1
		Bt-caspase-3b	XP_018914007.1
IAPs			
Diptera	*Drosophila melanogaster*	dBruce	NP_001262460.1
		Deterin	NP_650608.1
		DIAP1	NP_524101.2
		DIAP2	NP_477127.1
	Aedes aegypti	AaeIAP6	XP_021713190.1
		AaeIAP5	XP_001648266.1
		AaeIAP1	XP_021695484.1
		AaeIAP2	XP_021705807.1

Table S5. Oligonucleotides used in this study.

Target	Name	Sequence 5'-3'	Orientation
Primers for RT and qRT-PCR			
Ap-Ark	Ap-Ark-F	TCGAAGGCTTGGATCAATGGT	Forward
	Ap-Ark-R	TGCAATTTCAGACTGTACACGG	Reverse
Ap-Dronc-1	Ap-Dronc-1-F	ACTGCAATACGTGATCCAATAGA	Forward
	Ap-Dronc-1-R	CATCAATCTAGCCAATTCGGTATTA	Reverse
Ap-Dronc-2	Ap-Dronc-2-F	GGCATACTGCTAAACGTGATCC	Forward
	Ap-Dronc-2-R	TGCATTCAATTCAGTGTTATAGGCA	Reverse
Ap-ICE-1	Ap-ICE-1-F	ACATGGTAACCACGATACAAACAC	Forward
	Ap-ICE-1-R	AGTGTCCTTGCCAGGTTGAT	Reverse
Ap-ICE-2	Ap-ICE-2-F	GCAACTCCGTAACTACAAACTGC	Forward
	Ap-ICE-2-R	AAAAGCGTCGGCAGTGTCA	Reverse
Ap-Decay-1	Ap-Decay-1-F	ACACGGTCTTCTTCAGGCAG	Forward
	Ap-Decay-1-R	TTGAGTTGGTCGGGCATCAA	Reverse
Ap-Decay-2	Ap-Decay-2-F	ATTGTTGTGTTGACACACGGG	Forward
	Ap-Decay-2-R	AGTTTAGGTTTTCCGGCTAGTGT	Reverse
Ap-IAP-A1	Ap-IAP-A1-F	GTTCCCGATTCGATGTTGTGC	Forward
	Ap-IAP-A1-R	CACACAGCACACTGTTCGAG	Reverse
Ap-IAP-A2	Ap-IAP-A2-F	CCCTTGTCTTCACACCATTGC	Forward
	Ap-IAP-A2-R	TCTTTGACGTTTTCTTCGTCCA	Reverse
Ap-IAP-A3	Ap-IAP-A3-F	TGAAAGTGGCTTGTGTCCCT	Forward
	Ap-IAP-A3-R	CAGGTCCATCGGCTGTCTAC	Reverse
Ap-IAP-A4	Ap-IAP-A4-F	CCAAGGTCTGATGGATTGGGA	Forward
	Ap-IAP-A4-R	TTCACCACCAACCTCTTCCAC	Reverse
Ap-IAP-B1	Ap-IAP-B1-F	CGTCGTTTGAAAGAAGCCCG	Forward
	Ap-IAP-B1-R	AGTAGCCTTGATGGTCTGTCG	Reverse
Ap-Deterin-1	Ap-Deterin-1-F	GAACCCCTTCAACACATCTGG	Forward
	Ap-Deterin-1-R	CTGCTTCGGCCATATCCTTG	Reverse
Ap-Deterin-2	Ap-Deterin-2-F	AAATGGCCGAAGCAGGTTTTT	Forward
	Ap-Deterin-2-R	AAGGCTGGTCAGTTGGCTC	Reverse
Primers for gene amplification prior to Gateway cloning (sequences corresponding to attb1 and attb2 tail are underlined)			
Ap-IAP-A1	Ap-IAP-A1-attb1	GGGGACAACTTTGTACAAAAAAGTTGGCACCATGTCCAACGGATGCCCG	Forward
	Ap-IAP-A1-attb2	GGGGACAACTTTGTACAAGAAAGTTGGCAACTATAAGTACACTTGTATGGTGG	Reverse
Ap-IAP-A2	Ap-IAP-A2-attb1	GGGGACAACTTTGTACAAAAAAGTTGGCACCATGATAAAGGTTCATTCCCA	Forward
	Ap-IAP-A2-attb2	GGGGACAACTTTGTACAAGAAAGTTGGCAACTATAAGTACACTTGTATGG	Reverse
Ap-IAP-A4	Ap-IAP-A4-attb1	GGGGACAACTTTGTACAAAAAAGTTGGCACCGAAATATTTGGCACCGC	Forward
	Ap-IAP-A4-attb2	GGGGACAACTTTGTACAAGAAAGTTGGCAACTATAAGAACACTTGCATAT	Reverse
Ap-IAP-B1	Ap-IAP-B1-attb1	GGGGACAACTTTGTACAAAAAAGTTGGCACCATGGAATCGCCACAGTCA	Forward
	Ap-IAP-B1-attb2	GGGGACAACTTTGTACAAGAAAGTTGGCAATTAAGAAAGGAATGTACGAAC	Reverse
Ap-Deterin-1	Ap-Deterin-1-attb1	GGGGACAACTTTGTACAAAAAAGTTGGCACCATGGAGAACATCGACAACGT	Forward
	Ap-Deterin-1-attb2	GGGGACAACTTTGTACAAGAAAGTTGGCAATCATGACATTCCCTTTTTTTGG	Reverse

Dataset legends

Dataset S1 (separate file). Similarity between *Acyrthosiphon pisum* and *Drosophila melanogaster* caspase protein sequences.

Dataset S2 (separate file). Similarity between *Acyrthosiphon pisum* and *Drosophila melanogaster* IAP protein sequences.